⊕EPA # Project Summary

NAPL: Simulator Documentation

Joseph Guarnaccia, George Pinder, and Mikhail Fishman

A mathematical and numerical model is developed to simulate the transport and fate of NAPLs (Non-Aqueous Phase Liquids) in near-surface granular soils. The resulting three-dimensional, three phase simulator is called NAPL. The simulator accommodates three mobile phases: water, NAPL and gas, as well as water- and gas-phase transport of NAPL contaminants. The numerical solution algorithm is based on a Hermite collocation finite element discretization. Particular attention has been paid to the development of a sub-model that describes three-phase hysteretic permeability-saturation-pressure (k-S-P) relationships, and that considers the potential entrapment of any fluid when it is displaced. In addition rate-limited dissolution and volatilization mass transfer models have been included. The overall model has been tested for self-consistency using mass balance and temporal and spatial convergence analysis. The hysteretic k-S-P and mass exchange models have been tested against experimental results. Several example data sets are provided, including a setup of the artificial aquifer experiments being conducted at the EPA's Subsurface Protection and Remediation Division of the National Risk Management Research Laboratory in Ada, OK.

This Project Summary was developed by EPA's National Risk Management Research Laboratory's Subsurface Protection and Remediation Division, Ada, OK, to announce key findings of the research project that is fully documented in a separate report of the same title (see Project Report ordering information at back).

INTRODUCTION

The physical problem which is addressed is the contamination of a pristine porous medium as the result of releases of organic liquids, commonly referred to as Non-Aqueous Phase Liquids (NAPLs), in near-surface heterogeneous granular soils. The organic liquids can be either lighter than water or heavier than water. The soil domain is idealized as consisting of three interrelated zones: a vadose zone which is in contact with the atmosphere, a capillary fringe zone, and a water-table aquifer zone. A particular problem of interest may include all three zones or a subset thereof. Granular soils are stable (non-deforming) and relatively chemically inert (the soil particles do not interact with the soil fluids). Therefore, the soil is idealized as containing a high percentage of quartz particles and only a minor percentage of clay particles and organic matter.

A conceptual illustration of surface-release-generated NAPL migration in the vadose, capillary fringe and aquifer zones is provided in Figure 1. There are three fundamental mechanisms for NAPL migration. First, the NAPL infiltrates into the soil and migrates both vertically and laterally under the influence of gravitational and capillary forces. The distribution of the NAPL liquid is a function of fluid properties (density, viscosity, interfacial tension, wetting potential and variable chemical composition), soil properties (grain size distribution, mineral content, moisture content, porosity, hydraulic conductivity and spatial heterogeneity), and system forcing history. If the source is periodic in nature, then during drying periods, not all the NAPL will drain from the pore space, leaving
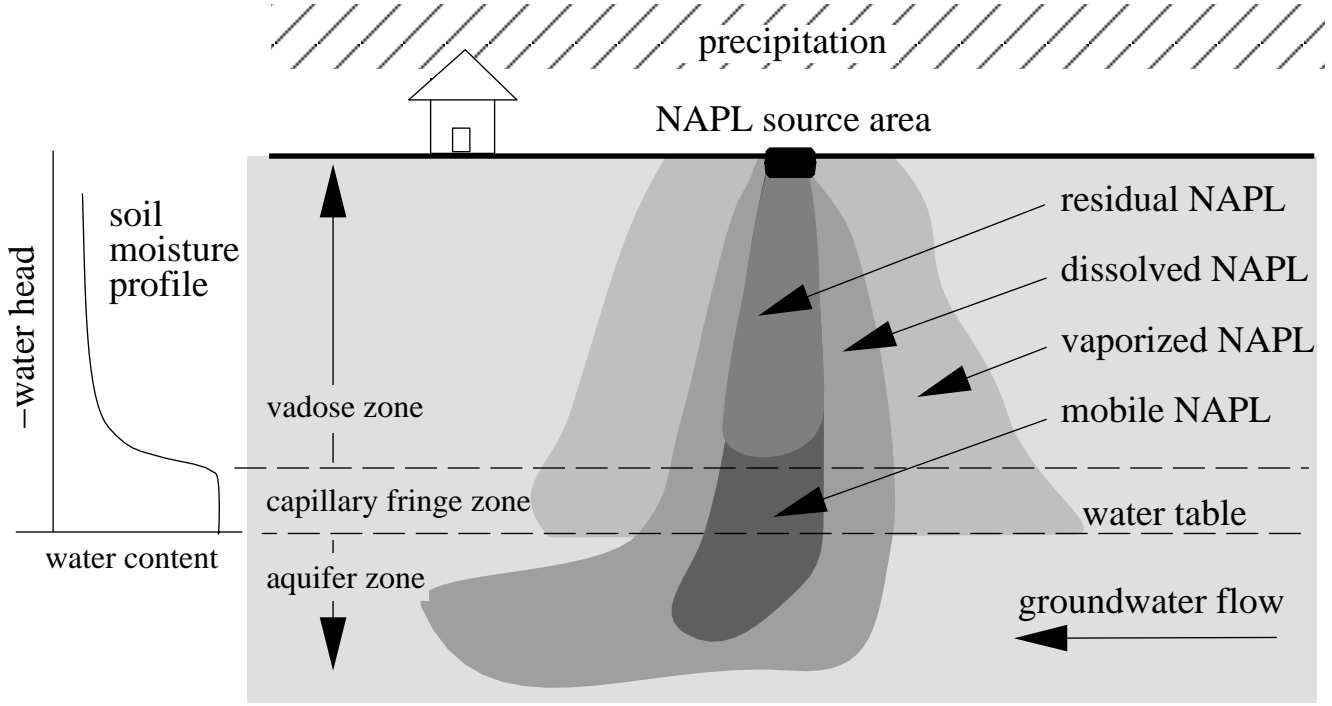
Figure 1. *Definition illustration of NAPL contamination in near-surface soils due to an intermittent release.*

behind an immobile residual, held in place by capillary forces. If the NAPL is more dense than water, it will migrate through the capillary fringe and continue its vertical migration until either the mobility becomes zero (all the NAPL liquid is at the immobile residual state) or the NAPL front encounters an impenetrable geologic horizon.

The second contaminant transport mechanism is dissolution and consequent advection in the downward-flowing water-phase, with precipitation providing the water source in the vadose zone. In the case of a DNAPL, flowing ground water picks up dissolved NAPL constituents.

The third transport mechanism is transport as a vapor NAPL constituent in the soil gas, where the increased gas-phase density induces downward movement. Partitioning between the gas- and water-phase contaminants further enhances the migratory potential of the NAPL constituents.

DESCRIPTION OF MODEL

Mathematical Statement of the Model NAPL

The model NAPL is designed to solve the following system of governing equations along with initial and boundary conditions.

Mass Balance Equations

Following the development of Pinder and Abriola (1986), the mass balance law for each fluid constituent, an ordered pair (i,a) representing a species i in a fluid phase is:

$$\frac{\partial\left(\varepsilon S_\alpha \rho_i^\alpha\right)}{\partial t} + \nabla\cdot\left[\varepsilon S_\alpha \rho_i^\alpha \upsilon^\alpha\right] - \nabla\cdot$$

$$\left[\varepsilon S_\alpha \rho_i^\alpha \upsilon^\alpha D^\alpha \cdot \nabla\left(\frac{\rho_i^\alpha}{\rho^\alpha}\right)\right] + \varepsilon S_\alpha \kappa^\alpha \rho_i^\alpha = \rho_i^\alpha Q^\alpha + \hat{\rho}_i^\alpha$$

(1)

where the *five* constituents (i,a) relevant to this simulator are identified as: (w,W), a water species in the water phase;(n,W), a NAPL species in the water phase; (n,N), a NAPL species in the NAPL phase; (n,G), a NAPL species in the gas phase; and (g,G), a gas species in the gas phase.
Other symbols occurring in equation 1 are used to represent the following:
ε is the porosity of the porous medium.
S_a is the saturation of the a-phase.
r_i^a is the mass concentration of species in the a-phase [M/L^3].
n^a is the mass average velocity of a-phase, a vector [L/T].
D^a is the dispersion coefficient for the a-

phase, a symmetric second-order tensor [L^2/T].
Q^a is the point source(+) or (-) a-phase mass [$1/T$].
k_i^a is the decay coefficient for species in the a-phase [$1/T$].
$\hat{\rho}_i^\alpha$ is the source or sink of mass for a species in the a-phase [M/L^3T] due to interphase mass exchange (i.e., dissolution, volatilization and adsorption).
The exchange of mass for each constituent in equation 1 is defined by:

$$\hat{\rho}_w^W = 0$$
$$\hat{\rho}_n^W = E_n^W - E_{n/w}^G - E_{n/w}^S$$
$$\hat{\rho}_n^N = -\left(E_n^W + E_n^G\right)$$
$$\hat{\rho}_n^G = E_n^G + E_{n/w}^G$$
$$\hat{\rho}_g^G = 0$$

(2)

where

E_n^W represents dissolution mass transfer of NAPL species from the NAPL phase to the water phase;

2

$E_{n/w}^{G}$ represents volatilization mass transfer of the NAPL species from the water phase to the gas phase;

E_{n}^{G} represents volatilization mass transfer of the NAPL species from the NAPL phase to the gas phase;

$E_{n/w}^{S}$ represents adsorption mass transfer of the NAPL species from the water phase to the soil.

A sixth mass balance equation is required to describe the NAPL species mass which is adsorbed onto the soil. This equation is written as:

$$\frac{\partial\left([1-\varepsilon]\rho^{S}\omega_{n}^{S}\right)}{\partial t}+[1-\varepsilon]\rho^{S}\kappa_{n}^{S}\omega_{n}^{S}=E_{n/w}^{S}$$

(3)

where

ρ^{S} is the density of the soil [M/L^3] and

ω_{n}^{S} is the mass fraction of the adsorbed NAPL on the solid [dimensionless].

The balance of equation 3 is replaced by the following linear equilibrium relationship:

$$\omega_{n}^{S}=K_{d}\,\rho_{n}^{W} \qquad (4)$$

where

K_{d} is a distribution coefficient [L^3/M].

To ensure global mass conservation, the following definitions and constraints on fluid volume, density and mass exchange are employed:

1. The a-phase saturations must sum to one:

$$S_{W}+S_{N}+S_{G}=1 \qquad (5)$$

2. The a-phase mass density [M/L^3] is the sum of the species mass concentrations in the a-phase:

$$\rho^{\alpha}=\sum_{\iota=w,n,g}\hat{\rho}_{\iota}^{\alpha},\ \alpha=W,N,G \qquad (6)$$

3. The sum of mass fluxes of all species into the a-phase must equal the total mass change in the a-phase:

$$\hat{\rho}^{\alpha}=\sum_{\iota=w,n,g}\hat{\rho}_{\iota}^{\alpha},\ \alpha=W,N,G \qquad (7)$$

4. The total mass change over all phases must be zero:

$$\sum_{\alpha=W,N,G}\hat{\rho}^{\alpha}=0 \qquad (8)$$

5. The sum of the reacting mass must be equal to the sum of the produced mass:

$$\sum_{\iota=w,n,g}\kappa_{\iota}^{\alpha}\rho_{\iota}^{\alpha}=0,\ \alpha=W,N,G \qquad (9)$$

A set of fluid phase mass balance equations can be generated by summing the balance equation 1 for each species within the phase, and by incorporating equations 2,6 and 7. The three resulting fluid-phase mass balance equations are:

Water-phase:

$$\frac{\partial\left(\varepsilon S_{W}\rho^{W}\right)}{\partial t}+\nabla\cdot\left[\varepsilon S_{W}\rho^{W}v^{W}\right]$$
$$=\rho^{W}Q^{W}+E_{n}^{W}-E_{n/w}^{G}-E_{n/w}^{S}$$

(10)

NAPL-phase:

$$\frac{\partial\left(\varepsilon S_{N}\rho^{N}\right)}{\partial t}+\nabla\cdot\left[\varepsilon S_{N}\rho^{N}v^{N}\right]$$
$$=\rho^{N}Q^{N}-E_{n}^{W}-E_{n}^{G}$$

(11)

Gas-phase:

$$\frac{\partial\left(\varepsilon S_{G}\rho^{G}\right)}{\partial t}+\nabla\cdot\left[\varepsilon S_{G}\rho^{G}v^{G}\right]$$
$$=\rho^{G}Q^{G}+E_{n}^{G}+E_{n/w}^{G}$$

(12)

With this development, the physical problem can be cast into a mathematical representation consisting of five mass balance equations. Of the balance equations written, the following five are used in the simulator:

1 to 3) The three fluid-phase balance equations, equations 10,11 and 12. These equations define the temporal and spatial distribution and the flow properties of the water-, NAPL- and gas-phases throughout the domain.

4 and 5) The two NAPL species balance equations, equation 1 with (i,a) = (n,W) and

(n,G). These equations define the temporal and spatial distribution of the NAPL species as they are transported within and between their respective phases.

PHASE ADVECTION

Fluid flow is defined by the parameter v^a in equations 1 and 10 through 12. The phase velocity is written in terms of the multi phase extension of Darcy's law.

$$v^{\alpha}=-\frac{k\,k_{r\alpha}}{\varepsilon S_{\alpha}\mu^{\alpha}}\cdot\left(\nabla P^{\alpha}-\gamma^{\alpha}\nabla z\right),$$
$$\alpha=W,N,G$$

(13)

where

P^{α} is the a-phase pressure [$M/(LT^2)$],

$\gamma^{\alpha}=\rho^{\alpha}g$ is the specific weight of the phase [M/T^2],

g is the acceleration due to gravity [L/T^2],

k is the intrinsic permeability [L^2], considered a scalar herein, and

k_{ra} is the relative permeability.

The a-phase relative permeability is a scaling factor, $0\le k_{r\alpha}\le 1$, which accounts for the case where the porous medium is not fully saturated with the a-phase. This parameter is in general a function of the a-phase saturation. Given the assumption that the phase wetting-order is constant, and follows, from most to least, water-NAPL-gas, the following functional dependance is assumed:

$$k_{rW}=k_{rW}\left(S_{W}\right)$$
$$k_{rN}=k_{rN}\left(S_{W},S_{Tw}\right)$$
$$k_{rG}=k_{rG}\left(S_{Tw}\right)$$

(14)

where the relationships listed reduce to their proper two-phase forms when appropriate. The form of equation 13 for each fluid phase of interest is detailed here as:

$$v^{W}=-\frac{kk_{rW}}{\varepsilon S_{W}\mu^{W}}\cdot\left(\nabla P^{W}-\gamma^{W}\nabla z\right)$$

$$v^{N}=-\frac{kk_{rN}}{\varepsilon S_{N}\mu^{N}}\cdot\left(\nabla\left(P^{W}+P_{cNW}\right)-\gamma^{N}\nabla z\right)$$

(15)

$$v^{G}=-\frac{kk_{rG}}{\varepsilon S_{G}\mu^{G}}\cdot\left(\nabla\left(P^{W}+P_{cNW}+P_{cGN}\right)-\gamma^{G}\nabla z\right)$$

MASS TRANSFER

Four types of mass transfer processes are important in defining the physics of the fate of NAPLs in near surface granular soils:

(a) dissolution mass transfer of pure phase NAPL to the water phase;

(b) evaporation mass transfer of pure phase NAPL to the gas phase;

(c) evaporation mass transfer of NAPL species in the water phase to the gas phase;

(d) adsorption mass transfer of NAPL species in the water phase to the soil phase.

Adsorption of NAPL species in the gas phase directly to the soil phase is neglected.

Liquid-Liquid Mass Transfer

When the organic phase is at an immobile residual state, saturation is no longer considered a function of capillary pressure since capillary pressure becomes undefined. Consider the NAPL phase balance equation 11 for the case of an immobile residual with constant phase density, constant porosity, and no external sources or sinks. For these conditions equation 11 reduces to:

$$\varepsilon \rho^N \frac{\partial S_N}{\partial t} = -E_n^W - E_n^G \quad \textbf{(16)}$$

This equation states that change in NAPL saturation is due to mass transfer processes.

The dissolution model defining the mass exchange term, E_n^W, is assumed to be a first-order kinetic-type reaction of the form:

$$E_n^W = C_n^W \left(\overline{\rho}_n^W - \rho_n^W \right) \quad \textbf{(17)}$$

where

C_n^W [1/T] is the rate coefficient which regulates the rate at which equilibrium is reached, and

$\overline{\rho}_n^W$ [M/L^3] is the equilibrium concentration of the NAPL species in the water phase (solubility limit).

In the simulator $\overline{\rho}_n^W$ is assumed to be a measurable constant value.

To determine the parametric form of C_n^W, the work of Imhoff et al. (1992) is employed. They conducted column experiments designed to study dissolution kinetics of residual trichloroethylene (TCE) in a uniform sand by flushing the system with clean water and tracking the dissolution front as a

function of time. Using a lumped parameter model, they derived the following power-law relationship for C_n^W:

$$C_n^W = \beta_1^{WN} \left(\varepsilon S_N \right)^{\beta_2} \left| v^W \right|^{\beta_3} \quad \textbf{(18)}$$

where

$$\beta_2 \approx 0.5$$
and
$$\beta_3 \approx 1.0$$

are dimensionless fitting parameters. The parameter β_1^{WN} [1/T] is the rate coefficient, and it is fit to available experimental- or field-scale data.

The volatilization model defining the mass exchange term E_n^G is assumed to follow a similar model as for dissolution, i. e.:

$$E_n^G = C_n^G \left(\overline{\rho}^G - \rho_n^G \right) \quad \textbf{(19)}$$

where

C_n^G [1/T] is the rate coefficient which regulates the rate at which equilibrium is reached, and

$\overline{\rho}_n^G$ [M/L^3] is the constant equilibrium vapor concentration of the NAPL species in the gas phase (vapor solubility limit).

The rate coefficient C_n^G is assumed to have the form:

$$C_n^G = \beta_1^{GN} \left(\varepsilon S_N \right)^{\beta_2} \quad \textbf{(20)}$$

where

β_2 is the same as for the dissolution model, and

β_1^{GN} [1/T] is fit to available data.

Consider now the volatilization of a dissolved NAPL species in the water phase to the gas phase. Assuming that the water phase is at residual saturation in the vadose zone, and that there are no external sources or sinks of mass, then equation 10 can be written as:

$$\varepsilon S_W \frac{\partial \rho^W}{\partial t} = E_n^W - E_{n/W}^G - E_{n/W}^S \quad \textbf{(21)}$$

where

the exchange term E_n^W is defined in equation 15 and $E_{n/W}^G$ governs the volatilization mass transfer of a dissolved NAPL species in the water phase to the gas phase:

$$E_{n/W}^G = C_{n/W}^G \left(H\rho_n^W - \rho_n^G \right) \quad \textbf{(22)}$$

where

H is the dimensionless Henry's law coefficient which is defined at equilibrium conditions as follows:

$$H = \rho_n^G / \rho_n^W \quad \textbf{(23)}$$

and

$C_{n/W}^G$ [1/T] is the mass transfer rate coefficient which is assumed to be defined by the power law:

$$C_{n/W}^G = \beta_1^{GW} \left(\varepsilon S_w \right)^{\beta_2} \quad \textbf{(24)}$$

where

the fitting parameter β_2 is assumed to be the same as for the liquid-liquid mass transfer models, and β_1^{GW} [1/T] is fit to the available data.

Liquid-Solid Mass Transfer

Finally, mass exchange due to adsorption, $E_{n/W}^S$ is assumed to be defined by a linear equilibrium model:

$$\omega_n^S = K_d \rho_n^W \quad \textbf{(25)}$$

where

K_d is the distribution coefficient [L^3/M] defined as a function of the organic carbon content of the soil and the relative hydrophobicity of the dissolved NAPL species:

$$K_d = f_{oc} K_{oc} \quad \textbf{(26)}$$

where

f_{oc} is the mass fraction of organic carbon and

K_{oc} is the organic carbon partition coefficient. Combining equations 3 and 25 yields the following definition for $E_{n/W}^S$:

$$E_{n/W}^S = \rho^b K_d \left(\frac{\partial \rho_n^W}{\partial t} + \kappa_n^S \rho_n^W \right) \quad \textbf{(27)}$$

where

$\rho^b = \left[1 - \varepsilon \right] \rho^S$ is the bulk density of the soil.

MODEL TESTING AND EXAMPLE PROBLEMS

A series of pseudo-one-dimensional example problems were presented in order to evaluate convergence and mass balance, and to give the user an indication of appropriate discretization for a given set of input data. In addition to addressing self-consistency, four example problems were designed to simulate specific physical experiments:

1. a three-phase LNAPL spill and redistribution experiment (Van Geel and Sykes, 1995a, 1995b);

2. a three-phase DNAPL spill and redistribution experiment conducted at the EPA's Subsurface Protection and Remediation Division of the National Risk Management Research Laboratory in Ada, Oklahoma;

3. an experimental investigation of the dissolution of residual DNAPL in a saturated sand (Imhoff et al, 1992);

4. an experimental investigation of DNAPL vapor transport in an unsaturated sand (Lenhard et al., 1995).

The first example simulates water drainage in a one-dimensional soil column, 1.2 meters long and initially saturated with water. The boundary conditions are: at the top, open to the atmosphere, and at the bottom, specified water head (fine sand = 10 cm, coarse sand = 60 cm). The columns are then allowed to drain under the influence of gravity until quasi-static conditions prevail. Figure 2 presents the results for the simulation in the first example.

The second example is summarized as follows:

1. For time = 0 to 100 s, DNAPL is rejected at a constant volume rate of 0.03 cm^3/s

2. for time = 100 s to the end of the simulation, P^G = atmospheric.

Simulation results for two different discretizations are presented in Figure 3. A time step of order 2 seconds was required to obtain a solution for this problem, as larger time steps caused convergence problems. Figure 3 shows the total liquid saturation solution at initial conditions (T = 0) and at T = 200 s (100 s after the DNAPL source was removed). One can see that while both discretizations capture the sharp DNAPL front, the x = 2.5 cm solution exhibits oscillations behind the front. Figure 3 presents saturation results at time = 5000 s, after the DNAPL has migrated to near static, residual state. It is apparent that for

these model parameters, a grid spacing of approximately 1 cm is required. Figures 3.2c and 3.2d present mass balance results for this simulation. In general the model performs well with respect to mass balance except when boundary forcing is changed, and several time steps are needed to accommodate the discontinuity imposed.

Mass Transfer Model

Here we investigate the convergence attributes of the kinetic mass transfer model. Consider the following one-dimensional water flow and contaminant transport problem. The initial conditions are set such that the domain is saturated, and there is a zone of residual DNAPL, $S_N = 0.15$, uniformly distributed from x=25 cm to the bottom. The boundary conditions are set such that there is a constant influx of clean water at the top at a rate of 0.008 cm/s, and an equivalent efflux of contaminated water at the bottom. Relevant mass transfer and transport parameters are:

$$\beta_2 = 0.5,$$

$$\beta_3 = 1.0,$$

and

$$a_L^W = 1\,cm,$$

and

$$\overline{\rho}_n^W = 0.001\,gm/cm^3.$$

The results for different values of the exchange rate coefficient, β_1^{WN}, are presented in Figures 4a and 4b. As shown in the Figure, a distinct dissolution front is created, the shape of which is a function of the size of β_1^{WN}. High values effectively approximate the equilibrium partitioning approximation and produce a sharp front, while low values produce a broad front. From a numerics standpoint, the dissolution front should be resolved over several elements to minimize oscillations in the solution which can cause erroneous NAPL saturations upstream of the source area.

Spatial convergence is illustrated in Figures 4c and 4d. For a constant rate coefficient, $\beta_1^{WN} = 24/d$, the model exhibits convergence as the mesh is refined.

BIBLIOGRAPHY

Imhoff, P.T., P.R. Jaffe, and G.F. Pinder, An experimental study of the dissolution of trichloroethylene in saturated porous media, Princeton University Water Resources Program Report: WR-92-1, 1992.

Lenhard, R.J., M. Oostrom, C.S. Simmons, and M.D. White, Investigation of density-dependent gas advection of trichloroethylene: Experiment and a model validation exercise, J. Contaminant Hydrology, 19, 47-67, 1995.

Pinder, G.F., and L.M. Abriola, On the simulation of nonaqueous phase organic compounds in the subsurface, Water Resour. Res., 22 (9), 109s-ll9s, 1986.

Van Geel, P.J., and J.F. Sykes, Laboratory and model simulations of a LNAPL spill in a variable-saturated sand medium: 1. Laboratory experiment and image analysis techniques, Journal of Contaminant Hydrology, 17(1), 1-26, 1995a.

Van Geel, P.J. and J.F. Sykes, Laboratory and model simulations of a LNAPL spill in a variable-saturated sand medium: 2. Comparison of laboratory and model results, Journal of Contaminant Hydrology, 17(1), 27-53, 1995b.
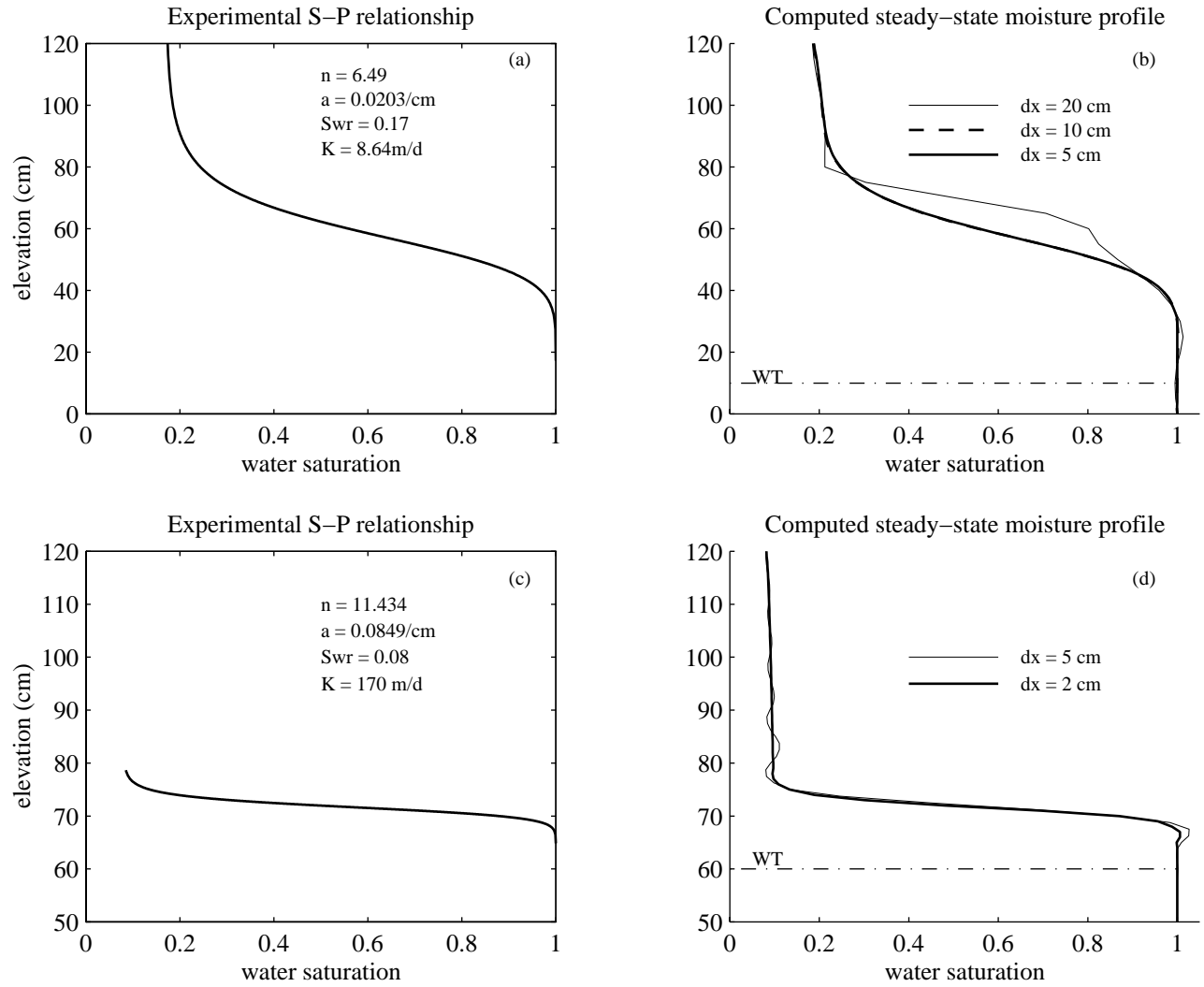
Figure 2. *Analysis of appropriate grid spacing to compute capillary rise for different soil-types. Parts (a) and (b) are for a relatively fine sand, and parts (c) and (d) are for a relatively coarse sand.*
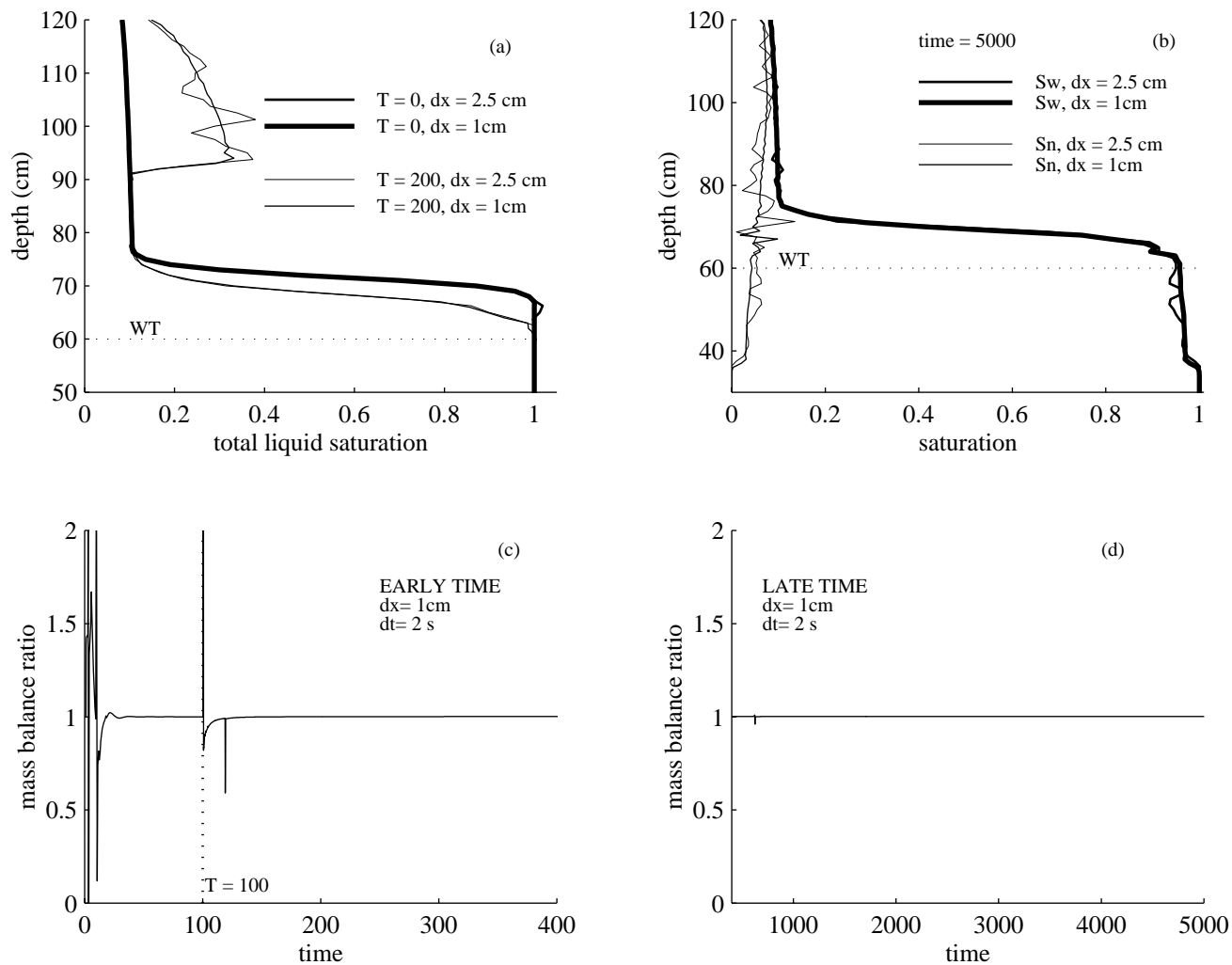
Figure 3. *Results of a one-dimensional, three-phase, DNAPL injection and redistribution simulation, highlighting spatial convergence and mass balance.*
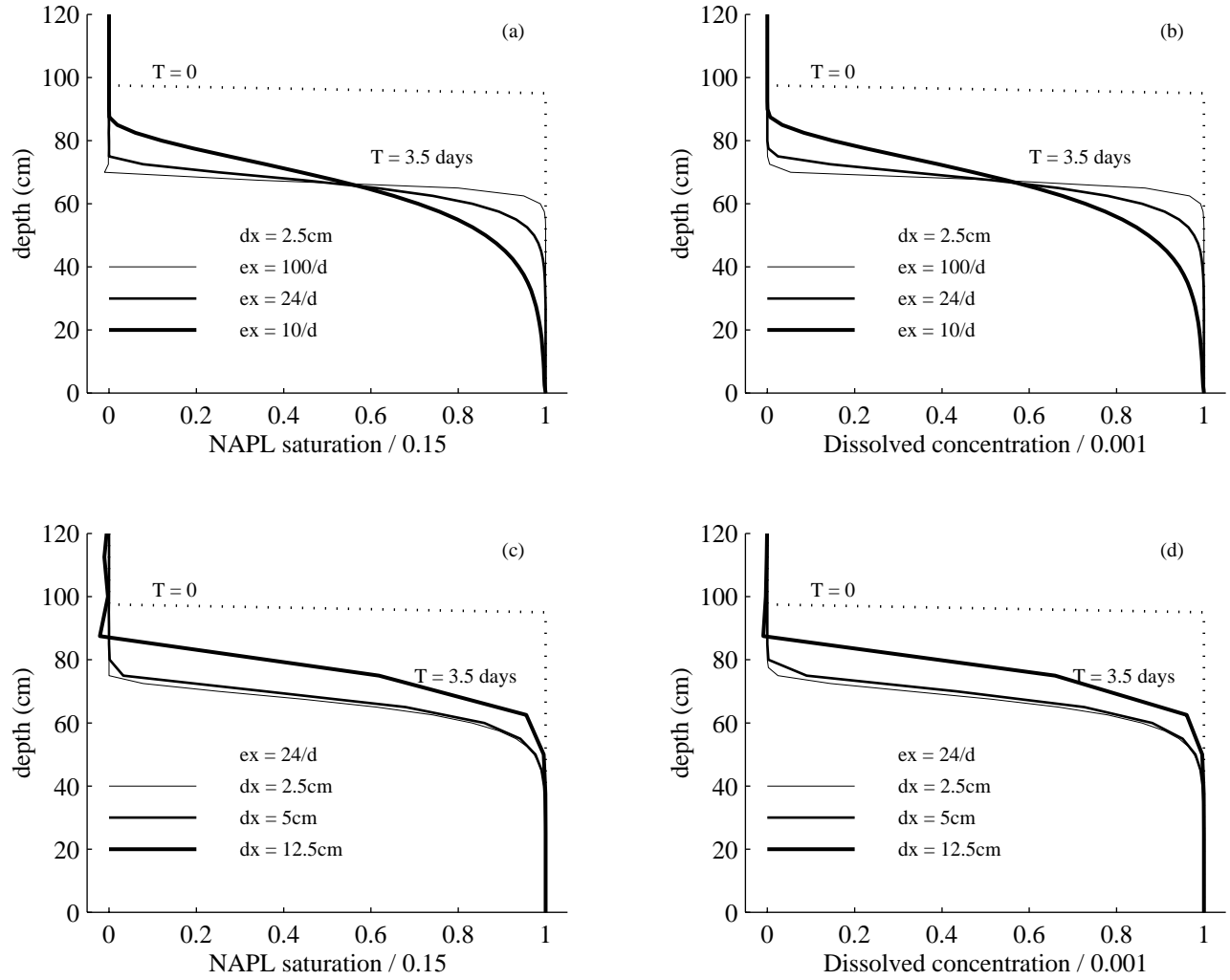
Figure 4. *Computational analysis of the dissolution model. Parts (a) and (b) illustrate the effect that the rate constant has on the solution. As the dissolution front sharpens, oscillation appears indicating that a finer grid spacing is required. Parts (c) and (d) illustrate spatial convergence for ex=24/d. For the parameters chosen a grid spacing of approximately 5 cm is appropriate.*

United States
Environmental Protection Agency
Center for Environmental Research Information
Cincinnati, OH 45268

Official Business
Penalty for Private Use
$300

EPA/600/SR-97/102

BULK RATE
POSTAGE & FEES PAID
EPA
PERMIT No. G-35